

# Refractories: Controlled microstructure composites for extreme environments

W. E. LEE, S. ZHANG

*Department of Engineering Materials, University of Sheffield, Mappin St., Sheffield, S1 3JD, UK*

*E-mail: w.e.lee@sheffield.ac.uk*

M. KARAKUS

*Department of Ceramic Engineering, University of Missouri-Rolla, 222 McNutt Hall, Rolla, MO 65409-0330, USA*

Techniques for the examination of refractories microstructures are described with particular emphasis on the need to use a range of techniques from TEM, FEGSEM, SEM to optical microscopy and macroscale to cover all magnification scales. The grain and bond and composite nature of most powder processed refractories is emphasised and illustrated with examples of microstructural evolution on firing and in service and corrosion when in contact with silicate slags. In particular the use of cathodoluminescence in conjunction with reflected light microscopy for rapid and broad scale phase recognition is highlighted.

© 2004 Kluwer Academic Publishers

## 1. Introduction

### 1.1. Refractories production and types

Refractories are composite materials used in large volumes in extreme, usually corrosive, environments as furnace linings for high temperature materials processing and other applications in which thermomechanical and thermochemical properties are critical [1]. Significant consumers of refractories are the glass melting, cement and ceramic industries each using about 8% of production. However, by far the greatest user is the iron and steel industry consuming about 65% of production. Types of refractories range from relatively dense (up to 90%) bricks to low density (10%) fibrous thermal insulation. Refractories may be fabricated and sold shaped (e.g., as bricks) or unshaped (monolithics or fibres).

Shaped (brick) manufacture is most often from powder mixtures commonly combining many different material types such as ceramic (oxide) powders, graphite flakes and polymer resins to form the final product. The powders have a large particle size distribution (PSD) enabling small (sub- $\mu\text{m}$ ) particles to pack in the gaps between large (up to several mm) particles so that most of the densification occurs during the shape forming operation. This is unlike most engineering ceramics where most densification occurs in the sintering step. Unfired, powder processed, refractories are often 85% dense. Processing from large PSD powders leads to a complicated microstructure composed of large, discrete aggregate (filler) refractory grain particles held together by a continuous bonding matrix often containing extensive porosity, a so-called grain and bond microstructure [2]. A common feature of such a microstructure is microcracking from thermal expansion mismatch of different phases, and from sintering of the

fine particle fraction causing shrinkage and opening up cracks between the larger particles which do not sinter as rapidly. If smaller than the critical flaw size such microcracks provide useful toughening, increasing resistance to crack propagation and improving thermal shock resistance. Refractory blocks are also made from molten liquids produced in electric arc furnaces (EAF) that are poured into graphite moulds and cooled slowly over several days. Such a process gives a microstructure much like a cast metal for these fused cast (electrocast or electrofused) refractories. Crystallization from the melt and subsequent grain growth leads to interlocked grains that may be up to several mm long. Low levels of porosity and little glassy phase may result from this route so that fused blocks are used in applications where extreme chemical resistance is required since liquid ingress is limited by such a microstructure.

Unshaped material can be installed and shaped *in-situ*. Such monolithics include castables (sold as dry mix which, when mixed with water, can be shaped by casting or vibrating, the hydraulic cement chemical bond forms at room temperature and converts to a physical ceramic bond on firing), or as gunning mixes (flowing mixtures specially made for placing by pneumatic or mechanical projection), or as mouldables or plastics (in a plastic “clay” form which can be rammed into position and fired *in-situ* to give a ceramic bond although these are less popular as their installation cannot be easily mechanised). Once installed and fired monolithic refractories have typical grain and bond microstructures although porosity levels in the bond may be higher than in fired bricks. Refractories are also made in lump or ground form (aggregate/grain) or as fibre wool and shapes (such as mats and felts). Highly porous (<30%

## CHARACTERISATION OF CERAMICS

dense) refractories such as fibre shapes are termed low thermal mass (LTM). Unshaped monolithic and LTM materials account for over 50% of refractories usage.

Fired brick or monolithic refractories invariably contain many phases each of which provide useful properties or enable the processing to be performed. The aggregate/grain phases in different systems do not vary much, commonly being fused or sintered  $\text{Al}_2\text{O}_3$ ,  $\text{MgO}$  and spinel ( $\text{MgCr}_2\text{O}_4$ ,  $\text{MgAl}_2\text{O}_4$ ). Where these refractories do differ is in the bonding systems used, which include ceramic, cement and carbon types. These may e.g., be ceramic bonds derived from clay which on firing leaves mullite and an aluminosilicate glass or from fine additions of  $\text{Al}_2\text{O}_3$ ,  $\text{MgO}$  and  $\text{SiO}_2$  reacting to form mullite, spinel and glass. In monolithics, where a castable or gunning slurry is installed which must then set or harden and dry, hydratable cement bonds typically based on calcium aluminate cements are used. These undergo hydration reactions forming e.g.,  $\text{CAH}_{10}$  and  $\text{C}_2\text{AH}_8$  (the cement shorthand is used where C = CaO, A =  $\text{Al}_2\text{O}_3$  and H =  $\text{H}_2\text{O}$ , subscripts indicate number of moles) on mixing with water that lead to setting after installation and then react at high temperature to give a ceramic bond. Carbon bonds derived from pyrolysis of pitch or phenolic resin binders form in oxide-carbon refractory bricks used extensively in primary steelmaking operations.

These materials are true composites in that each constituent contributes useful behaviour to the system. For example, in oxide-carbon refractories the oxide confers oxidation resistance and refractoriness while the graphite provides increased thermal conductivity, non-wetting behaviour (to hot metal and slag) and slag resistance. Since oxide and graphite would react at high temperatures a third phase is required to bond them, this is the carbon derived from the pitch or resin. The softening of the resin or pitch at relatively low temperatures enables the batch to flow facilitating shape forming. Once shaped pyrolysis of the binder leaves fine carbon, which also has the beneficial properties of graphite, listed above. As another example, the clay used in ceramic bonded refractories enables control of the rheology and shaping operations even though the aluminosilicate glass resulting from its decomposition degrades high temperature properties. Similarly, the cement bond in castable and gunning monolithics enables these installation procedures to be performed before hydration is encouraged. Often metal is added to refractories such as stainless steel fibres in monolithics which improve thermal shock resistance by acting as crack arresters, or Si or Al powder added to  $\text{MgO}$ -C bricks to improve oxidation resistance and high temperature strength. A major advantage of C-bonded refractories is their ability to use different grain materials in different parts of a component but retaining the common carbon bond. For example, in oxide-C hollowware for continuous casting of steel  $\text{ZrO}_2$  or  $\text{MgO}$  is used in the high wear contact regions while cheaper  $\text{Al}_2\text{O}_3$  grain is used elsewhere (Section 2.4). The use of such a composite system is possible since the grain materials are effectively inert upon firing and the carbon bond derives only from the resin/pitch binder.

In LTM refractories it is the porosity which confers useful properties such as permeability or low thermal conductivity and can be considered a vital part of the composite structure.

### 1.2. Hierarchies or scales of microstructure

When considering which technique to use to examine any ceramic microstructure it is important to decide what resolution is required. The resolution of the technique used to examine a refractory brick where minor impurities may have no effect on relevant properties will be much less than for a critical electroceramic sensor component whose properties may be controlled by ppm levels of dopant. Furthermore, the scale of examination may be important in revealing different levels of uniformity from macro to micro scale. If a component is divided into 20 equal volume units and the composition and phase distribution, grain size, porosity and texture of each volume is determined to be the same in each unit then the component can be said to be uniform with respect to these characteristics on this scale of size. Repeating the experiment for 200 units may show up nonuniformity on a finer scale. In general to fully understand a microstructure it is necessary to examine at all levels of magnification. Just examining using an optical microscope will reveal the coarsest flaws which may be the most significant in a refractory brick but just using a transmission electron microscope (TEM) to examine a nanoceramic may mean any gross flaws are missed and it is these which may be critical. The techniques used must be governed by the application and properties desired in the ceramic. Furthermore, to fully characterise a complex microstructure requires that a range of techniques be used to determine the phases present, their crystal structures, their texture (i.e., the relation of the coarse grains or aggregates to the bond and porosity) and morphology. Fig. 1 shows the macro-to nano-scales which need to be considered when using  $\text{MgO}$ -C bricks in a Basic Oxygen Steelmaking vessel. In such a demanding application they are all important. Any modelling of refractories microstructures of the sort already being applied to Portland cement systems [3] needs to include all levels of the structure.

Optical microscopy remains not only the easiest but also the most important method for refractories characterisation. The resolution limit of about  $0.2 \mu\text{m}$  can be regarded as an advantage since, without it, an overall impression of the microstructure is not gained. For example, grain size and pore distributions are best conducted on as large an area as possible. Cathodoluminescence (CL) spectroscopy in conjunction with optical [4] or electron [5] microscopy is a useful tool for examination of refractories. In this technique a high energy (10–20 kV) electron beam is scanned over the specimen surface which on interaction either with trace amounts of activators in the sample such as transition metal ( $\text{Mn}^{2+}$ ,  $\text{Cr}^{3+}$ ) or rare earth ( $\text{Sm}^{3+}$ ,  $\text{Tb}^{3+}$ ,  $\text{Dy}^{3+}$ ,  $\text{Er}^{3+}$ ) ions or with lattice defects, gives rise to visible light emission. Luminesced light of a particular wavelength usually associated with a specific phase can then be mapped and correlated with the normal image to

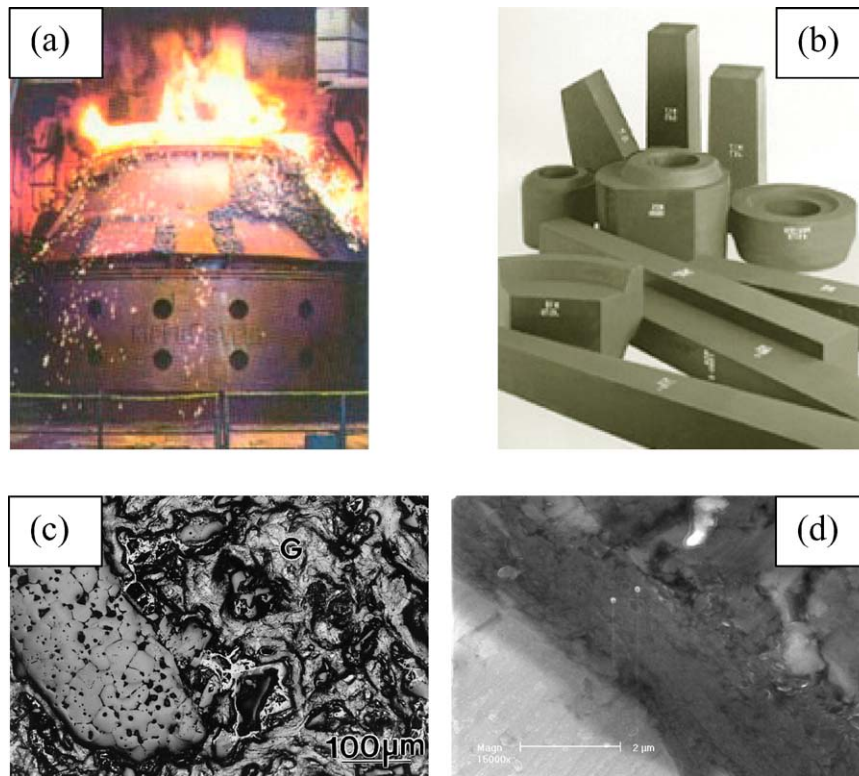


Figure 1 Showing the range of scales for MgO-C bricks used in a BOS vessel: (a) a ~5 m high BOS vessel, (b) ~1 m long MgO-C bricks showing their macroscale, (c) microscale in an SEM, and (d) nanoscale in a FEG-SEM.

reveal the location of the phase. In reflected light and SEM images phases in the complex assemblages of refractories may not be well distinguished. The high contrast formed in CL images provides easy phase and phase distribution recognition [6]. Furthermore, a single phase may show more than one CL colour due to the presence of trace levels of impurities arising from differences in the local micro-environment and indicative of their indiffusion or of local differences in atmosphere (oxidising or reducing). Such information is often not detectable in light or SEM images. SEM is used, however, for fractography and characterisation of the fine detail of the bond system (where even TEM has been used to examine direct bonding in magnesia-chromite refractories [7]). The Environmental SEM [8] is particularly useful, in conjunction with a heating stage, for *in-situ* examination of reactions involving solids and gases such as hydration of cements, corrosion and oxidation of carbides/nitrides and solids and liquids such as melting of grain boundary phases and slag attack of refractories.

One aspect of a ceramics microstructure which is often neglected in microscopy studies, but which can have enormous influence on both mechanical properties such as strength and electrical properties such as dielectric constant, is the porosity. The interconnected, open pore size distribution in a porous material, including powders, is most easily quantified using the technique of mercury porosimetry in which a holder is partially filled with a weighed, dried sample, evacuated and filled with Hg. Pressure applied to the nonwetting Hg causes penetration of pores greater than a particular size quantifiable through the Washburn equation. De-

tails of this technique are well described by Lowell and Shields [9].

A final feature of a microstructure that is difficult to characterise but which may have critical effects on properties is residual or internal stress. These are particularly important in refractories due to their multiphase nature. These elastic stresses arise from several sources including thermal stresses generated from the different thermal expansion coefficients of phases in the microstructure or within grains of non-isomorphous phases (i.e., excluding cubic crystals and glass), and mechanical stresses arising externally from abrasion or deformation (fabrication) processes or internally arising from e.g., polymorphic transformations with an associated volume change.

### 1.3. Microstructural evolution

Two approaches to refractories microstructural design have arisen. Initially, they were designed to be as close to equilibrium as possible after processing so that undesirable changes in use at high temperature (where of course the system tends to thermodynamic equilibrium) were avoided. More recently, refractories have been designed to alter in service by reaction either of phases in the refractories microstructure or with the furnace contents [10, 11]. Such *in situ* refractories may be defined as the in use product(s) of reaction within a refractory system or between the refractory system and furnace contents leading to improved refractory behaviour.

For a full understanding of the final fired microstructure of a refractory system it is strictly necessary to characterise the microstructures after each of the

## CHARACTERISATION OF CERAMICS

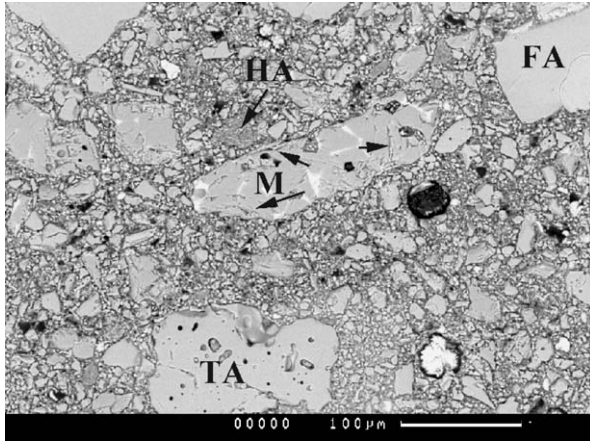


Figure 2 SEM image of a low cement castable containing a range of aggregate phases including tabular alumina (TA, note the closed porosity), white fused alumina (FA, note the lack of second phases) and sintered magnesia (M, with light contrast calcium and magnesium silicate second phases). HA is a hydratable alumina in the matrix. From ref. [12].

manufacturing stages. However, much useful information can be obtained by examining the evolution of the microstructure during the firing step or in use at high temperature, usually via studies of samples quenched from increasing temperatures. Sections 2.3 and 2.4 will describe some recent studies of microstructural evolution in refractories.

## 2. Refractories microstructures

### 2.1. Grain, aggregates or fillers

The microstructure of a typical refractory made by powder processing consists of grain and bond phases. Each of these will have undergone extensive synthesis before being incorporated into a brick. Typical grain materials include those made by melting or fusion (alumina, mullite, MgO, mullite/zirconia) and sintering (MgO, alumina, Mg aluminate spinel). Fused grain is expensive due to the high temperatures needed but pure since many (e.g., alkali) impurities volatilise during melting.

Sintered grain is cheaper and often has lower density but contains grain boundary impurities which are deleterious to high temperature properties. Refractory grain may also be derived from raw materials that have undergone less synthesis such as fireclays, flint clays, quartz, dolomite, graphite, bauxite, magnesite and members of the andalucite/kyanite/sillimanite group. These materials may have had relatively simple pre-processing after mining and beneficiation such as washing and calcination. Fused and sintered grain are easily distinguished since fused grain typically contains a lower proportion of second phases at grain boundaries and presents an even contrast in micrographs as illustrated in Fig. 2 (from [12]) for a low cement castable refractory. Bauxite is the ore used for production of alumina and aluminium and consists of aluminium hydroxides and oxide hydroxides along with a range of impurities (Na, Ti, Fe and Si). Calcination of bauxite produces a cheap, predominantly alumina, grain used extensively in steel-making refractories. Impurities such as  $\text{SiO}_2$ ,  $\text{TiO}_2$  and  $\text{Fe}_2\text{O}_3$  facilitate liquid phase sintering and form bonds between the alumina crystallites as well as occasional mullite (Fig. 3).

Fused alumina is produced in two forms: white and brown. White fused alumina is made from calcined Bayer alumina and different grades are available based on differences in alkali contents. It is used extensively in high-temperature refractory bricks and monolithics. Brown fused alumina is made from bauxite ore under conditions which allow the partial removal of impurities as ferrosilicon. The impurities left lower its melting temperature by about  $50^\circ\text{C}$  and it is commonly used e.g., in refractories for blast furnace trough and induction furnace linings. Tabular alumina grain is often  $>99\%$  pure and is produced by heating pellets of calcined alumina at temperatures  $>1925^\circ\text{C}$ , just below the melting temperature, until near 100% conversion of the fine,  $\alpha$ -alumina crystallites into large (40 to  $>200\ \mu\text{m}$ ) tablet-shaped crystals occurs. Tabular alumina crystals are hard and dense with good thermal conductivity and

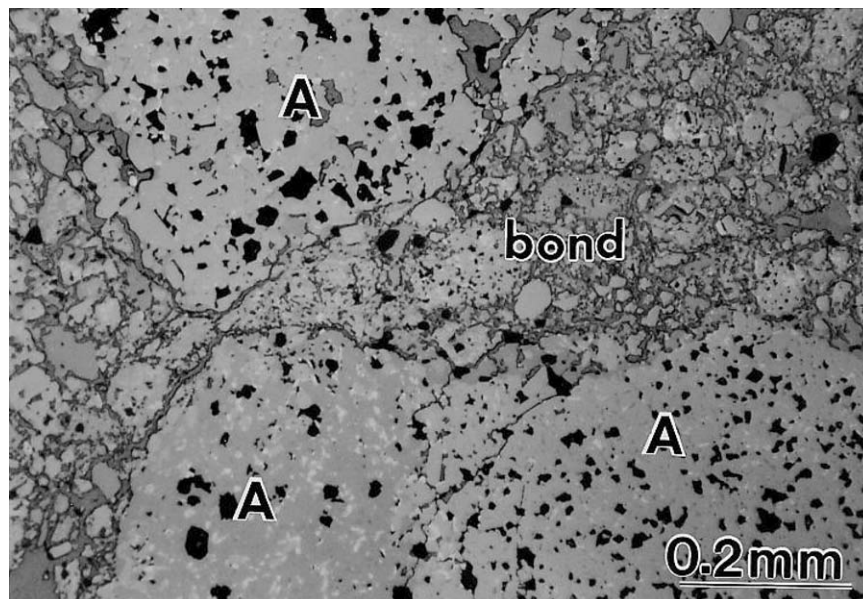


Figure 3 Reflected light image of high alumina refractory containing bauxite-derived grain (A) which is porous (dark), predominantly corundum  $\text{Al}_2\text{O}_3$ , but also contains lighter Fe- and Ti-containing phases which assist liquid phase sintering.

high crushing strength. However, they contain substantial closed porosity due to the large grain growth leaving pores in the centre of grains where volume diffusion is slow. Tabular aluminas are used extensively in alumina-graphite refractories, and in low-cement and ultra low cement castable mixes. Sintered MgO grain is available from magnesite ( $\text{MgCO}_3$ ) ore or derived from seawater. Dead burning or liquid phase sintering the fine MgO with e.g., CaO,  $\text{Fe}_2\text{O}_3$  and  $\text{SiO}_2$  to encourage grain growth and aggregate formation leaving less surface area available for reaction with moisture improves hydration resistance. Common second phases in dead burned magnesia are dicalcium silicate and forsterite.

A modern refractory system often contains a range of different grain materials to achieve the desired properties at as low a cost as possible. Fig. 2 shows a low cement castable (LCC) refractory containing sintered magnesia, fused alumina and tabular alumina grain.

## 2.2. Matrix or bond phases

Refractories are often characterised by the nature of their bond system. In silicate, glass or clay-bonded refractories the clay is often added as a powder, and with other, often aluminosilicate, phases such as fine alumina, sillimanite or andalucite ( $\text{Al}_2\text{O}_3\text{-SiO}_2$ ) forms the bond. In carbon-bonded oxide refractories the aggregate phases (typically MgO,  $\text{Al}_2\text{O}_3$  or  $\text{ZrO}_2$ ) are held together by a complicated bond system derived from decomposition of tar/pitch or phenolic resin binders. The nano-bond system in carbon-containing refractories is now attracting much attention [13]. In monolithic refractories the evolution of the bond system is more complicated since a hydraulic-type bond first forms at, or close to, room temperature soon after installation by e.g., casting or gunning techniques which is then fired to give a different high-temperature bond system. In aluminate-bonded oxide castable refractories the fine calcium aluminate cement powder (containing predominantly CA and  $\text{CA}_2$  phases) undergoes setting reactions to form hydrated phases such as  $\text{CAH}_{10}$  and  $\text{C}_2\text{AH}_8$ . Firing leads to dehydroxylation to  $\text{C}_{12}\text{A}_7$  above  $500^\circ\text{C}$  with CA and  $\text{CA}_2$  reappearing above about  $800^\circ\text{C}$  and eventual formation of  $\text{CA}_6$  above about  $1200^\circ\text{C}$  [14].

The matrix or bond system in a refractory is key both to the processing and properties of the product. The powders used are fine, usually  $<44\ \mu\text{m}$  and often nanoscale (Fig. 4) and so reactive. Their functions include: controlling rheology and so assisting installation (usually of wet systems) and packing, reacting to provide useful refractory phases at high temperature and reacting with the grain to provide strength to the fired product. Furthermore, matrix phases are often designed to react in service and provide protection to the composite. For example, metal additives (such as Al or Si) in oxide-C systems react with oxidising atmospheres protecting the carbon bond and generating ceramic phases (such as  $\text{MgAl}_2\text{O}_4$  or  $\text{Mg}_2\text{SiO}_4$ ), which improve high temperature strength.

Production of bond phase constituents typically involves more processing than that of grain phases. Aluminosilicate refractories to be used at low temperatures

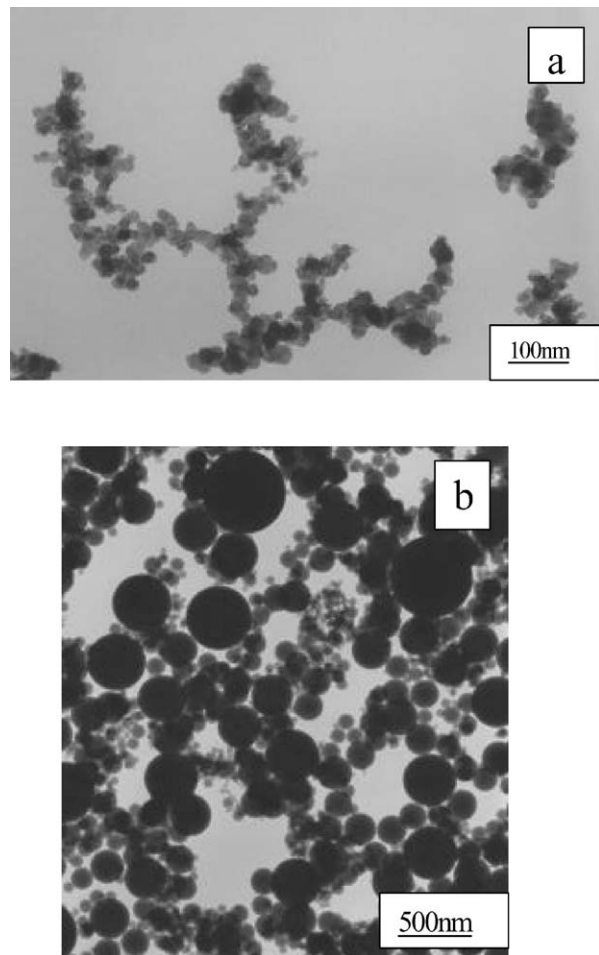


Figure 4 TEM images of nanoscale powders used in many refractory bond systems. a) Aggregated nano-carbon black (from reference 13) and b) fumed colloidal silica (courtesy of Dr. Peter Korgul, Sorby Centre for Electron Microscopy, University of Sheffield).

(< $1000^\circ\text{C}$ ) such as firebricks contain bond phases derived from reaction of clays with fine alumina to give a mullite/glass bond [15]. The carbon bond in oxide-C bricks is derived from a phenolic resin or pitch added as a binder during shape forming [16]. Decomposition of the pitch or resin leaves a fine, reactive carbon bond. Fig. 1d shows the nano-carbon matrix in a commercial resin-bonded MgO-C brick after firing 2 h at  $800^\circ\text{C}$  examined using a FEG-SEM. The detailed nature of the oxide-carbon bonding and its importance on refractory properties is poorly understood although it is now being examined using TEM [17]. Both FEGSEM and TEM suggest some interaction between the nano-carbon and the oxide grain (Fig. 5). Further the interaction of the carbon bond with other phases in the matrix such as the antioxidants described above or the grain phases is complex and highly dependent on local conditions [18].

The most common bond system in monolithic castables is based on calcium aluminate cements (CAC's) often with additional calcined Bayer (reactive) alumina and silica. CAC's are formed by reaction of lime and alumina either by a sintering or clinker process or from fusion [19]. The cements are predominantly CA and  $\text{CA}_2$  although minor  $\text{C}_{12}\text{A}_7$  may be present. Several grades of calcined Bayer process (in which  $\text{Al}(\text{OH})_3$  gibbsite is precipitated from dissolved



## CHARACTERISATION OF CERAMICS

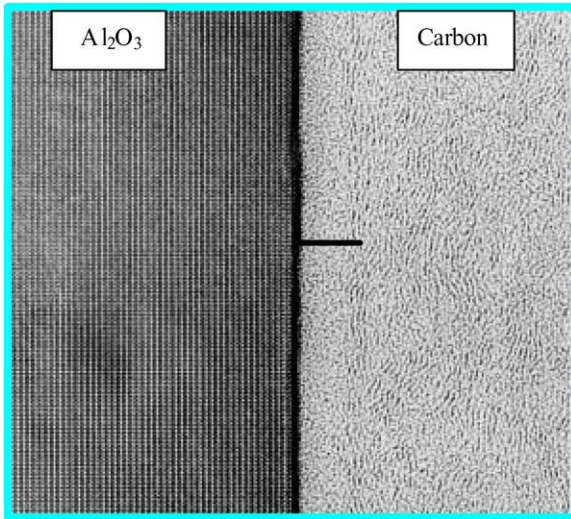


Figure 5 HREM image of the alumina-carbon interface in an alumina graphite refractory (from ref. 17). The alumina interplanar spacing in this image is 0.325 nm and the black horizontal line indicates the possible extent of oxide-C interaction.

bauxite ore) alumina are available. The level of soda impurity is critical since it leads to formation of Na  $\beta$ -alumina ( $\text{Na}_2\text{O}\cdot 11\text{Al}_2\text{O}_3$ ) on sintering which causes reduced density, strength, thermal shock and corrosion resistance. The colloidal silica used in refractory bond systems is a by-product of silicon manufacture and its spherical morphology (Fig. 4b) means it packs well and aids flow and so installation of monolithic refractories in which it is used extensively.

### 2.3. Microstructural evolution on firing

Since most densification is done prior to firing refractories the purpose of this operation is to bond together the phases in the microstructure to improve strength. In powder processed refractories the finer, more reactive, matrix phases react and bond the larger aggregate phases. This leads to strength development but since many different phases are present it may also leave high levels of residual stress, microcracking and gaps arising from thermal expansion mismatch. Such behaviour is, however, controlled to give the desired properties in the final product.

A good example illustrating the complexities of microstructural interactions on firing a refractory is provided by following *in situ* spinel formation in a LCC [20]. After firing at 1000°C the microstructure is similar to that observed after drying (Fig. 6a) containing cement and hydratable alumina agglomerates and fused and tabular aggregates as well as sintered MgO. After firing at 1200°C the microstructure changed considerably as low melting CaO-MgO- $\text{Al}_2\text{O}_3$ - $\text{SiO}_2$  (CMAS) phases led to liquid generation and spinel began to form on fine alumina particles in the matrix by reaction of the fine fractions (Fig. 6b). After firing at 1400°C the bond converted entirely to spinel with no alumina left in the matrix although some MgO remains (Fig. 6c). A few MgO grains located in silica-rich areas had forsterite ( $\text{Mg}_2\text{SiO}_4$ ) rims. Spinel formed with various morphologies including angular/faceted crystals (centre of Fig. 6c) and tuber-like (left side of Fig. 6c). After firing at 1500°C most MgO grains have been

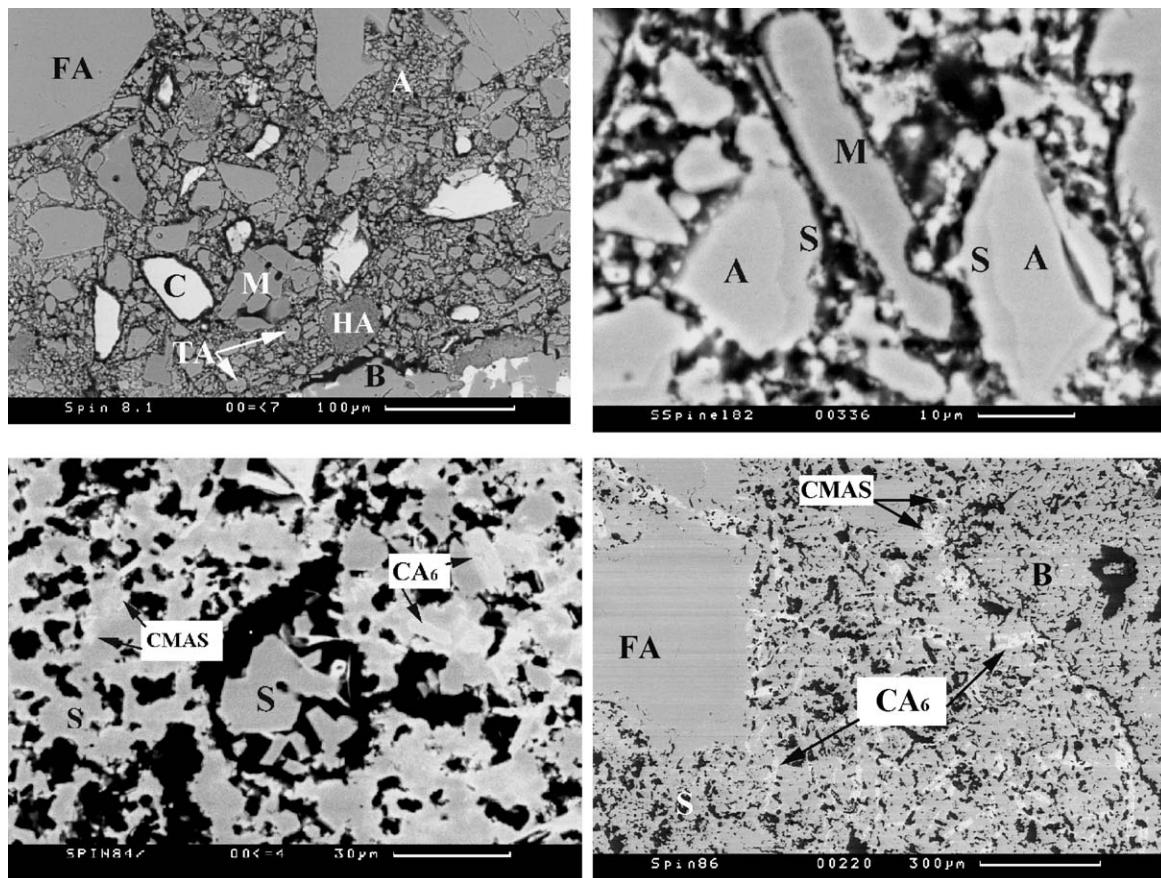


Figure 6 Backscattered SEM images of microstructural evolution of *in situ* spinel forming LCC: (a) dried at 110°C, and fired, (b) at 1200, (c) 1400 and (d) 1600°C. FA is fused alumina, B bauxite, C calcium aluminate cement, HA hydratable alumina, TA tabular alumina, S spinel and A alumina.

consumed except those covered by forsterite suggesting it protected them and delayed spinel formation. Spinel formation was completed after firing at 1600°C with no free magnesia detected. The microstructure (Fig. 6d) consisted of alumina grains surrounded by a spinel-rich matrix including some  $CA_6$  and CMAS (probably amorphous) containing small amounts of  $TiO_2$  and other impurities arising from the bauxite aggregates and MgO.

#### 2.4. Microstructural evolution in service

C-bonded bricks commonly used in primary steelmaking operations such as EAF and BOS are only given a low temperature (3–400°C) tempering treatment to stabilize the structure and remove volatiles before installation. They are then fired after placement in the use position. Various additives may also be made to them which react in service to give improved high temperature behaviour and oxidation resistance. Microstructural development thus occurs throughout their lifetimes, differently to silicate-bonded refractories where the firing treatment prior to use is usually designed to give a microstructure as close to equilibrium as possible so that ideally no further change occurs in service. Two types of additive are used in C-bonded-MgO refractories [21], metals/alloys such as Al, Si, Mg and Ca and boron-based compounds such as B,  $B_4C$ ,  $CaB_6$ ,  $ZrB_2$ ,  $Mg_3B_2O_6$  and  $SiB_6$ . These two additive types work in different ways. Metal/alloy additives act as CO reducing agents contributing to carbon oxidation inhibition and/or improving hot strength by forming high-temperature ceramic bonds such as  $Al_2O_3$  and  $Al_4C_3$  with Al metal addition. Fig. 7 shows the site of Al par-

ticles which have reacted to form oxides and carbides with differing morphologies in a MgO-C system [18]. Boron-based additives, on the other hand, act to block open pores to reduce the oxidation of carbon by formation of liquid phases. This has the drawback of lowering the hot strength. Carbon-containing refractories service lives in oxygen-rich atmospheres depend, to a large extent, on their oxidation resistance so that these additions have a critical function. Combinations of these two additive types may be used. Fig. 8 shows reflected light and CL images of a commercial MgO-C brick with Al+ $B_4C$  additives after firing at 1450–1500°C. These reveal extensive  $MgAl_2O_4$  spinel formation by reaction of the Al with host MgO but assisted by liquid derived from the  $B_4C$ . The amount of spinel formed is greater than when using only an Al additive.

A particularly useful aspect of C-bonded refractories is that various aggregates can be used in different areas of the body while maintaining the common carbon bond so the whole body can be given a single firing operation. For example, aggregates with improved wear behaviour can be used in areas of the component subject to severe wear conditions. In production of steel by continuous casting refractory 2 m long by ~0.2 m dia. stopper-rods are used to control the molten steel flow from ladle to tundish and tundish to mould. The tip or nose of these rods is subject to severe erosion and chemical attack and so the materials used must have good thermal shock properties and high chemical corrosion and spalling resistance. The major part of the rod is made of relatively cheap alumina-graphite but the high wear areas at the rod tip use e.g.,  $ZrO_2$  or MgO aggregates. Fig. 9 shows a high wear area of a refractory stopper containing both brown fused

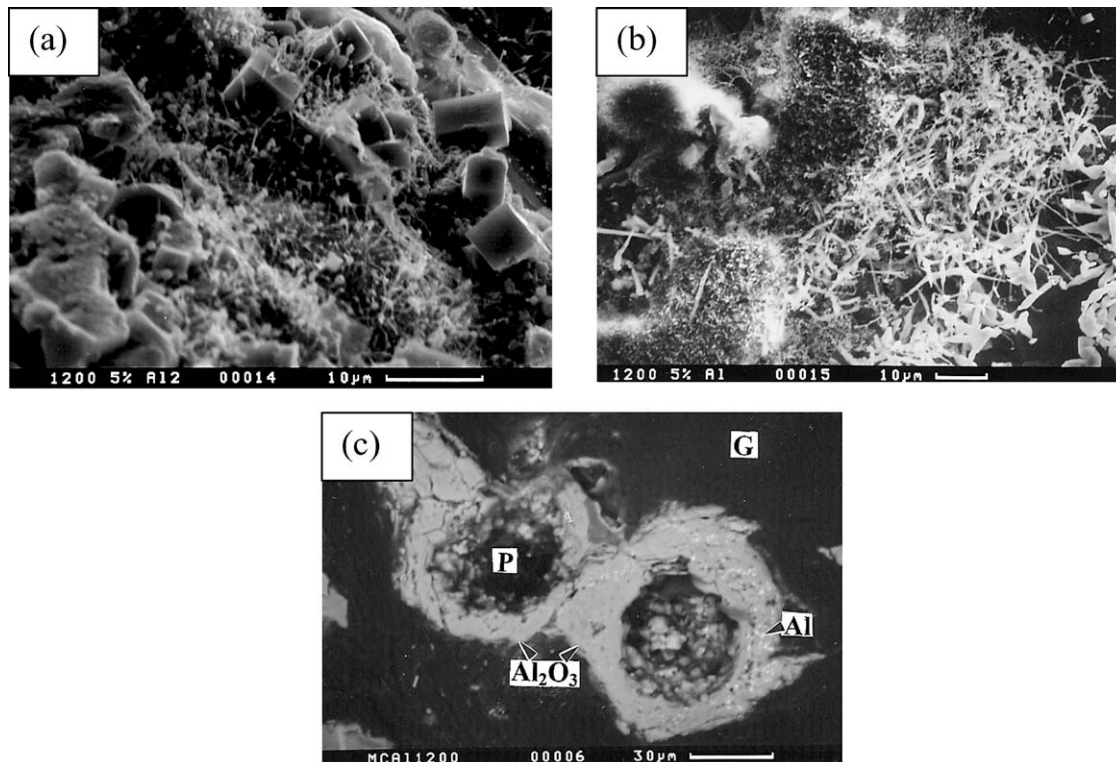
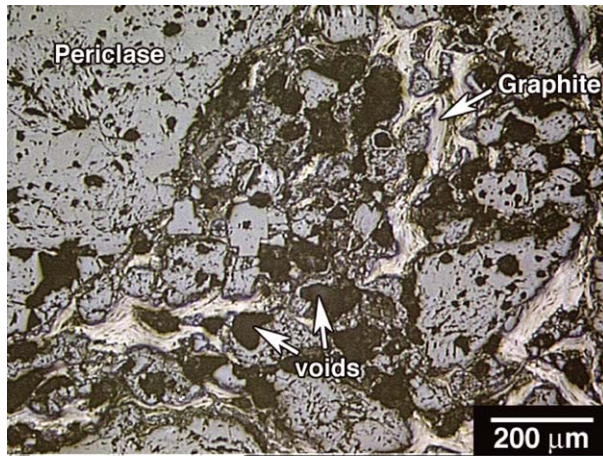


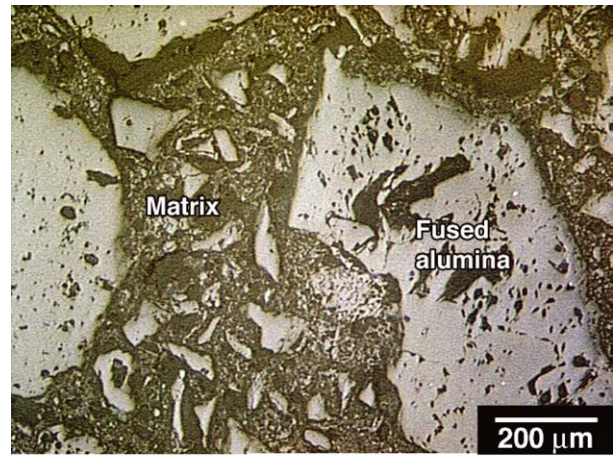
Figure 7 Morphologies of bonding phases formed from antioxidant Al metal particles in a MgO-C brick fired 3 h at 1200°C: (a) shows cuboidal spinel and AlN whiskers while, (b) shows AlN whiskers and fluffy  $Al_4C_3$  in top left while, and (c) shows an Al impregnated  $Al_2O_3$  shell around a pore (P) at the site of the original Al particles.



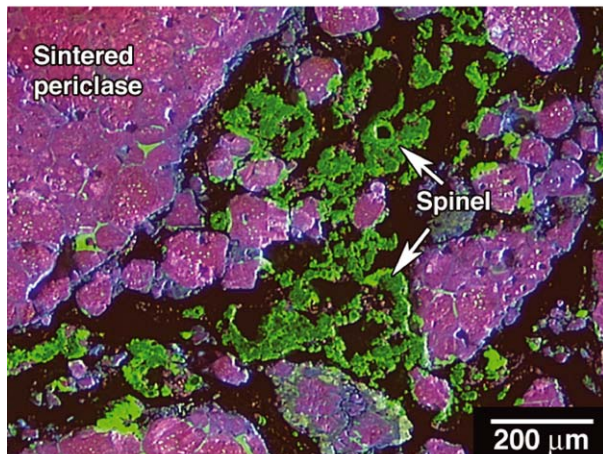
## CHARACTERISATION OF CERAMICS



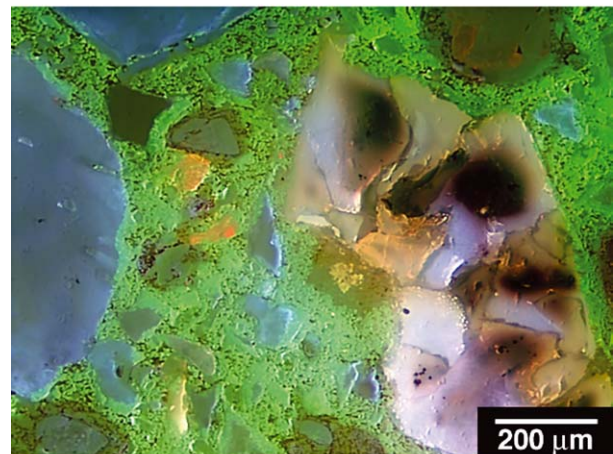
(a)



(a)



(b)



(b)

Figure 8 Reflected light (a) and CL image (b) showing extensive matrix spinel formation in MgO-C brick with added Al and B<sub>4</sub>C.

Figure 10 (a) Reflected light and (b) CL image of same area of a dry-vibratable castable revealing extensive matrix spinel (green CL) formation.

alumina and ZrO<sub>2</sub> in fused AZS (Al<sub>2</sub>O<sub>3</sub>-ZrO<sub>2</sub>-SiO<sub>2</sub>) grain. In addition depending on the particular steel being processed zirconia-graphite and magnesia-graphite stoppers are also used. The latter performs particularly well with Ca-Si treated steels.

Coreless induction furnaces for steelmelting are lined with dry-vibratable castable powder mixtures of alu-

mina aggregates and fine alumina and MgO that react *in situ* to form spinel. Fig. 10 shows reflected light and CL images of such a lining about 3 cm from the hot face in contact with the steel. The CL image reveals the full extent of spinel bond formation (green CL) while

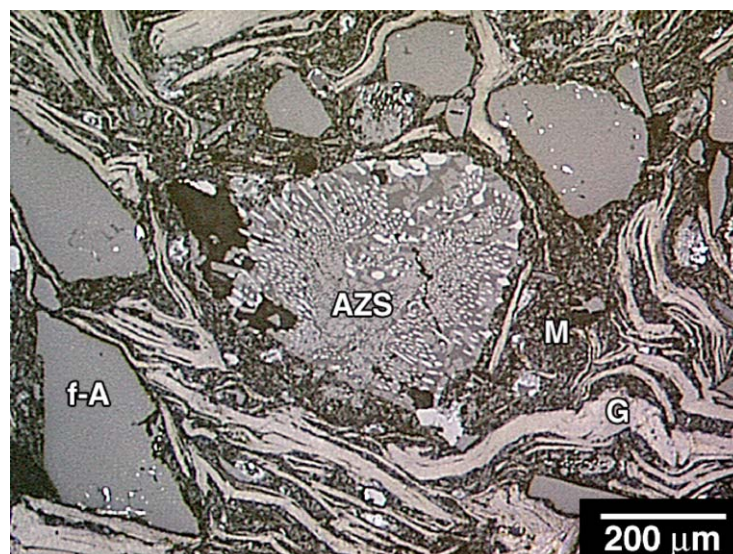


Figure 9 Reflected light image of high wear area of a refractory stopper rod showing several grain types (f-A is brown fused alumina, AZS is fused Al<sub>2</sub>O<sub>3</sub>-ZrO<sub>2</sub>-SiO<sub>2</sub>) in a single region. G are graphite flakes and M the fine alumina matrix.



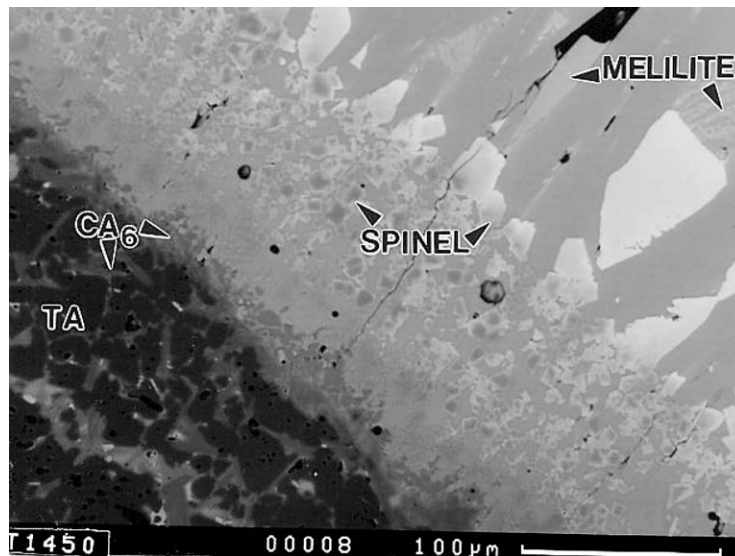


Figure 11 BSE image of tabular alumina (TA) grain after 1 h slag corrosion at 1450°C revealing a  $CA_6$  layer adjacent to the alumina while the slag (right) side contains angular, hercynitic spinel crystals that become brighter and richer in  $Fe_xO$  as they extend into the melilite-containing slag.

distinguishing the WFA (light blue CL) from the BFA (various CL colours such as yellow, red and white).

### 2.5. Corroded microstructures

Attack via matrix penetration by silicate slags and dissolution of solid phases is a major cause of refractories failure. Currently, studies of refractories corrosion involve applying the understanding obtained from attack of model systems using e.g., single crystals, binary slags and static tests to more complex and thus more realistic systems. This usually involves a static or dynamic corrosion test of a large grain or commercial refractory, detailed *post mortem* microstructural analysis and correlation to the expected thermodynamic phase equilibrium [22, 23]. The refractory-slag interface typically consists of several boundary layers or zones of attack including unaltered slag, a reaction zone (with massive changes in phase content compared to the orig-

inal refractory), a transition or intermediate zone (with some penetration and minor reaction) and unaltered refractory. Characterisation of the nature of these zones gives insight into the reaction mechanism.

Chemical attack of refractories by slags may be direct (congruent or homogeneous) and controlled by the reaction rate at the slag-refractory interface or the rate of diffusive transport of species to it through the slag leading to *active* corrosion. Indirect (incongruent or heterogeneous) attack, on the other hand, is controlled by diffusive transport through the slag or through a new solid phase, which forms at the original slag-refractory interface [22]. This may lead to *passive* corrosion. Several recent studies have examined corrosion of isolated commercial grain phases in model slags including fused and sintered MgO [24], white fused and tabular alumina [25], doloma and dolomite [26] and alumina-rich spinel and stoichiometric spinel [27]. Fig. 11 shows the emergence of calcium hexaluminate  $CA_6$  and spinel

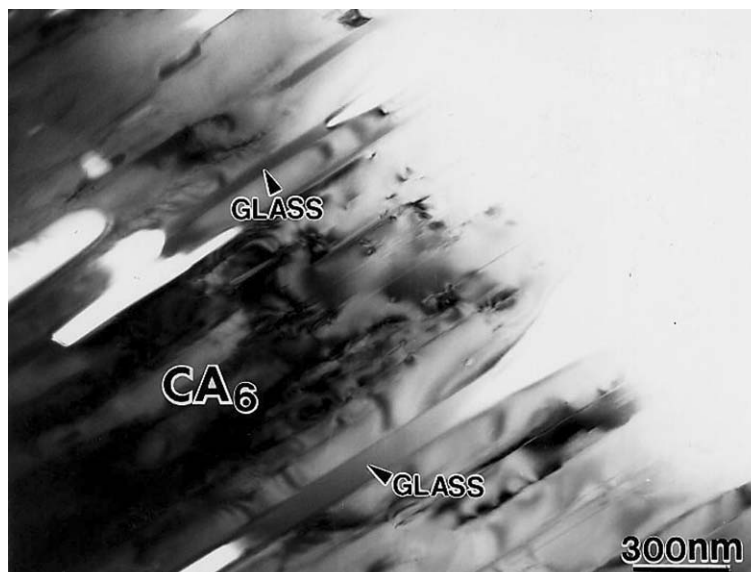


Figure 12 BF TEM image of a  $CA_6$  layer on WFA showing glass between the  $CA_6$  laths which would be liquid during corrosion suggesting some direct nature to the slag attack of this grain at 1450°C [24].

## CHARACTERISATION OF CERAMICS

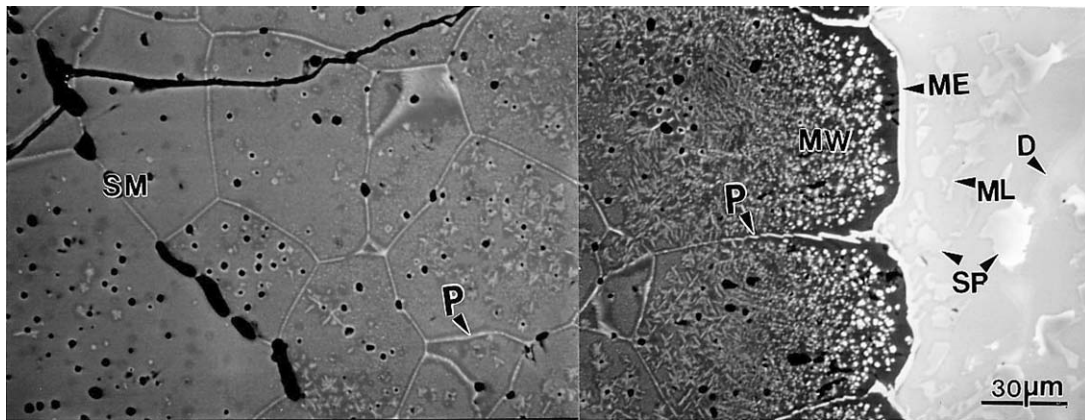
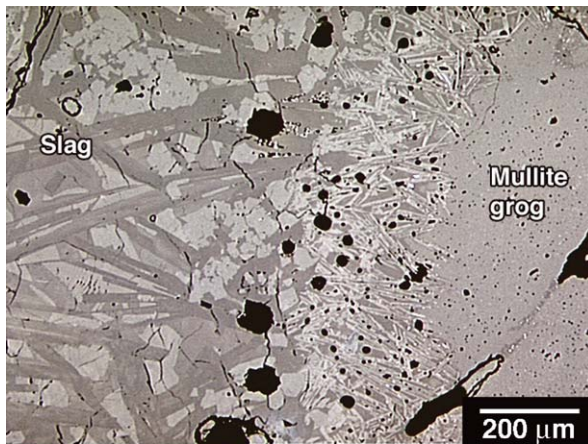


Figure 13 BSE image of sintered MgO grain (left side) corroded by EAF slag (right side) for 6 h at 1700°C showing slag penetration along grain boundaries (P), magnesiowustite layer (MW), merwinite (ME), melilite (ML), dicalcium silicate (D) and angular hercynitic spinel (SP).

layers on tabular alumina during a grain corrosion test at 1450°C in contact with a model  $\text{CaO-Al}_2\text{O}_3\text{-Fe}_x\text{O-SiO}_2$  slag indicating indirect corrosion [25]. Of particular note in this backscattered electron (BSE) image is the increasing brightness of the spinel crystals, indicative of increased  $\text{Fe}_x\text{O}$  content as they extend into the slag. This pick up of slag fluidising cations by the spinel makes the local slag more viscous and limits slag penetration so protecting the refractory. Bright-field TEM imaging of

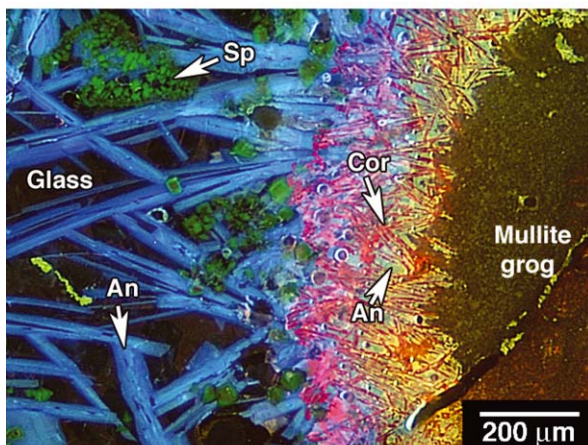
the  $\text{CA}_6$  layer formed on a white fused alumina (WFA) grain [25] in a similar corrosion test revealed glass between the  $\text{CA}_6$  laths. (Fig. 12) which would be liquid at the test temperature indicating some direct nature to the attack of WFA grain. Grain boundaries in sintered aggregates are vulnerable to attack and Fig. 13 shows extensive slag penetration in a sintered MgO grain after 6 h at 1700°C in contact with an EAF steelmaking slag [24].



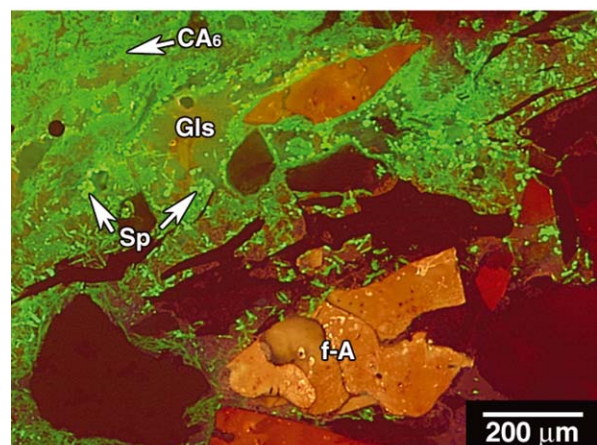
(a)



(a)



(b)



(b)

Figure 14 Attack of a 60% alumina castable. The mullite aggregate (grog) reacts with the liquid to form bright red CL prismatic corundum (Cor) crystals and a yellow CL anorthite (An) matrix while the slag has crystallized mostly to blue CL anorthite (An), green CL spinel (Sp) and glassy matrix.

Figure 15 Attack of a stopper rod by slag. Note the occlusion of fused alumina grain and graphite within the slag (Fig. 15a) while the CL image (Fig. 15b) reveals formation of glass (Gls), spinel (most intense green, euhedral crystals) and  $\text{CA}_6$  (bright green, acicular) at the slag-refractory interface.

Fig. 14 shows a low cost 60% alumina low cement castable as used in steel foundries which has been corroded by a CaO-MgO-Al<sub>2</sub>O<sub>3</sub>-SiO<sub>2</sub> slag. The CL image C clearly reveals corrosion of mullite grog (which is a mullite and cristobalite containing aggregate). The mullite is altered by the attack to prismatic corundum crystals and an anorthite matrix while the slag has crystallized to mostly anorthite and spinel in a glassy matrix.

Continuous casting stopper rods were described in Section 2.4. In ladles and tundishes, non-metallic inclusions accumulate on the stopper-rod surfaces, eventually reducing their service life. To limit non-metallic inclusion build-up and graphite loss, antioxidants (such as Si metal) are added to the refractory composition and Ar gas is provided to the nose of the stopper rods. Stopper-rods are preheated at 1200°C before casting so their surfaces are glazed with oxidation resistant glass compositions to reduce graphite loss during this operation. Fig. 15 shows attack of an AZS-reinforced Al<sub>2</sub>O<sub>3</sub>-graphite rod by ladle slag. Note the occlusion of fused alumina grain and graphite within the slag (Fig. 15a) while the CL image (Fig. 15b) reveals formation of glass, spinel and CA<sub>6</sub> at the slag-refractory interface.

### 3. Summary and conclusions

Refractories are complex multiphase materials used in some of the most severe conditions known to man. To understand their properties and structural evolution on processing needs a range of characterisation techniques to cover all possible length scales. This review has highlighted the use of optical and electron optical techniques in studies of microstructural evolution and corrosion.

### Acknowledgments

We dedicate this paper to the memory of Prof. R. E. Moore of the Department of Ceramic Engineering at Missouri-Rolla, USA.

### References

1. W. E. LEE, "Refractories" in Comprehensive Composite Materials Vol 4: Ceramic, Carbon and Cement Matrix Composites, edited by A. Kelly and C. Zweben (Elsevier, 2000) Chap. 4.12, p. 363.
2. W. E. LEE and W. M. RAINFORTH, "Ceramic Microstructures, Property Control by Processing" (Chapman and Hall, London, UK, 1994).
3. E. J. GARBOCZI, *Cem. Concr. Res.* **32** (2002) 1621.

4. D. J. MARSHALL, "Cathodoluminescence of Geological Materials" (Unwin Hyman, Boston, USA, 1988).
5. B. G. YACOBI and D. B. HOLT, "Cathodoluminescence Microscopy of Inorganic Solids" (Plenum Press, London, UK, 1990).
6. M. KARAKUS and R. E. MOORE, *J. Min. Mater. Char. Eng.* **1** (2002) 11.
7. K. GOTO and W. E. LEE, *J. Amer. Ceram. Soc.* **78** (1995) 1753.
8. G. D. DANILATOS, *J. Microsc.* **162** (1991) 391.
9. S. LOWELL and J. E. SHIELDS, "Powder Surface Area and Porosity" (Chapman and Hall, London, UK, 1984).
10. W. E. LEE and R. E. MOORE, *J. Amer. Ceram. Soc.* **81** (1998) 1385.
11. W. E. LEE, S. ZHANG and H. SARPOOLAKY, *Ceram. Trans.* **125** (2001) 245.
12. H. SARPOOLAKY, K. G. AHARI, J. MOLIN and W. E. LEE, in Proc. 44th Intl. Conf. on Refractories, Aachen, Germany (2001) p. 130.
13. S. TAMURA, T. OCHIAI, S. TAKANAGA, T. KANAI and H. NAKAMURA, in Proc. 8th Unified Intl. Tech. Conf. on Refractories (Unitecr) (Osaka, Japan, 2003) p. 517.
14. W. E. LEE, W. VIEIRA, S. ZHANG, K. G. AHARI, H. SARPOOLAKY and C. PARR, *Int. Mater. Revs.* **46** (2001) 145.
15. H. REZAIE, W. M. RAINFORTH and W. E. LEE, *Brit. Ceram. Trans.* **96** (1997) 181.
16. B. RAND and B. McENANEY, *Brit. Ceram. Trans. J.* **84** (1985) 158.
17. Y. MORIYOSHI, H. TANAK, T. IKEMOTO, T. ISHIGAKI and T. IKEGAMI, in Proc. 8th Unified Intl. Tech. Conf. on Refractories (Unitecr), (Osaka, Japan, 2003) p. 88.
18. S. ZHANG, N. J. MARRIOTT and W. E. LEE, *J. Euro. Ceram. Soc.* **21** (2001) 1037.
19. J. E. KOPANDA and G. MACZURA, in "Alumina Chemicals Science and Technology Handbook," edited by L. D. Hart (ACerS, 1990) p. 171.
20. H. SARPOOLAKY, K. G. AHARI and W. E. LEE, *Ceram. Intern.* **28** (2002) 487.
21. C. F. CHAN, B. B. ARGENT and W. E. LEE, *J. Amer. Ceram. Soc.* **81** (1998) 3177.
22. W. E. LEE and S. ZHANG, *Int. Mater. Rev.* **44** (1999) 77.
23. W. E. LEE, B. B. ARGENT and S. ZHANG, *J. Amer. Ceram. Soc.* **85** (2002) 2911.
24. S. ZHANG, H. SARPOOLAKY, N. J. MARRIOTT and W. E. LEE, *Brit. Ceram. Trans.* **99** (2000) 248.
25. S. ZHANG, H. R. REZAIE, H. SARPOOLAKY and W. E. LEE, *J. Amer. Ceram. Soc.* **83** (2000) 897.
26. Y. SATYOKO, W. E. LEE, E. M. PARRY, P. RICHARDS and I. G. HOULDSWORTH, *Ironmak. Steelmak.* **30** (2003) 203.
27. H. SARPOOLAKY, S. ZHANG and W. E. LEE, *J. Euro. Ceram. Soc.* **23** (2003) 293.

Received 20 August 2003

and accepted 20 January 2004